Article

J. Biol. Regul. Homeost. Agents. 2024; 38(5): 4349–4359
https://doi.org/10.23812/j.biol.regul.homeost.agents.20243805.345

Protecting Cerebral Blood Flow Autoregulation: A Frontier Study on Aripiprazole's Inhibition of the MAPK Signaling Pathway after Cerebral Ischemia

Jianghua Xu[1], Jie Zhu[2], Pengcheng Liu[3], Bin Ma[2,*], Tingyi Zhang[2,*]

[1]Neurology Department, Central Hospital Affiliated to Shandong First Medical University, 250000 Jinan, Shandong, China
[2]Neurointerventional Department, Jinan Zhangqiu District People's Hospital, 250200 Jinan, Shandong, China
[3]Neurology Department, Jinan Zhangqiu District People's Hospital, 250200 Jinan, Shandong, China
*Correspondence: mabin316536@163.com (Bin Ma); 674837108@qq.com (Tingyi Zhang)
Published: 1 May 2024

Background: Cerebral ischemia-reperfusion injury (CIRI) is a common severe complication following cerebrovascular diseases and poses significant challenges to human health and life. Aripiprazole, due to its unique pharmacological effects, is recognized to exert a protective effect against Ischemia/Reperfusion (I/R) injury. Therefore, this study aimed to explore the protective effect of Aripiprazole on CIRI by inhibiting the p38 mitogen-activated protein kinase (MAPK) signaling pathway and its impact on the function of cerebral blood flow autoregulation.

Methods: We successfully developed the CIRI rat model and divided rats into different groups: the Sham group, the I/R+DMSO group, the I/R+Aripiprazole low-dose group (1 mg/kg), and the high-dose group (3 mg/kg). The neuroprotective effect of Aripiprazole, its impact on the p38 MAPK signaling pathway, cell apoptosis, inflammatory response, oxidative stress response, and improvement of cerebral blood flow autoregulation function were evaluated using Triphenyltetrazolium Chloride (TTC) staining, western blot, terminal deoxynucleotidyl transferase dUTP Nick End Labeling (TUNEL) staining, and Enzyme-Linked Immunosorbent Assay (ELISA).

Results: Compared to the I/R+DMSO group, the I/R+Aripiprazole group exhibited a significant reduction in the volume of cerebral infarction, brain edema, neurological function injury scores, and the number of TUNEL-positive cells in brain tissue ($p < 0.05$, $p < 0.01$, and $p < 0.001$), indicating a significant neuroprotective effect of Aripiprazole. Western blot results revealed that Aripiprazole significantly inhibited the activation of the p38 MAPK signaling pathway induced by I/R ($p < 0.05$, $p < 0.01$, and $p < 0.001$). Additionally, Aripiprazole significantly reduced the expressions of pro-inflammatory cytokines (interleukin (IL)-1β, tumor necrosis factor-alpha (TNF-α), IL-6), decreased malondialdehyde (MDA) levels, and elevated the levels of superoxide dismutase (SOD) and glutathione (GSH) ($p < 0.05$, $p < 0.01$, and $p < 0.001$).

Conclusion: Aripiprazole effectively protects rats from CIRI by inhibiting the p38 MAPK signaling pathway, reducing cell apoptosis, suppressing inflammation and oxidative stress response, and improving cerebral blood flow autoregulation function. These findings provide an experimental basis for applying Aripiprazole in treating CIRI and lay the foundation for future clinical research.

Keywords: Aripiprazole; p38 MAPK pathway; CIRI; neuroprotection; cerebral blood flow autoregulation

Introduction

Cerebral ischemia poses a substantial threat to human health and life due to its high rate of morbidity and mortality [1]. Following an ischemia event, the affected area of the brain experiences cell death, resulting in nervous system impairment and inducing more severe secondary injuries [2]. Numerous pharmacological and cytological interventions aim to mitigate stroke-induced damage and enhance the recovery of neurological function in cases of sudden neurological dysfunction resulting from disrupted blood supply [3,4]. Cerebral Ischemia/Reperfusion (I/R) occurs when blood flow is restored after an ischemic phase [5]. Following I/R, the autoregulation of the cerebral blood vessels is essential for protecting nerve cells from damage. Therefore, it is crucial to investigate therapeutic targets and elucidate their protective mechanisms against cerebral ischemia [6].

In recent years, Aripiprazole has attracted attention due to its unique pharmacological effects [7]. While primarily used in the treatment of psychiatric disorders, Aripiprazole also shows promising potential in the field of neuroprotection [8]. Studies have indicated that Aripiprazole can influence various neurotransmitter systems, thus exerting neuroprotective effects [9,10]. The p38 mitogen-activated protein kinase (MAPK) signaling pathway is a critical mechanism for cellular response to stress and inflammation. Its activation during cerebral ischemia-

Journal of
BIOLOGICAL REGULATORS
and Homeostatic Agents

reperfusion injury (CIRI) is associated with various pathological processes, such as cell death, inflammatory responses, and oxidative stress [11–13]. Therefore, inhibiting the p38 MAPK signaling pathway may become an effective strategy for treating CIRI [14–16].

While studies have shown the potential neuroprotective effect of Aripiprazole, its specific mechanisms of action in CIRI, especially its effects on the p38 MAPK signaling pathway, remain unclear. Moreover, the impact of Aripiprazole on the autoregulation function of cerebral blood flow and its potential mechanisms have not been thoroughly studied. Therefore, exploring the mechanism by which Aripiprazole protects against CIRI and improves the autoregulation function of cerebral blood flow by inhibiting the p38 MAPK signaling pathway holds significant importance for developing new therapeutic strategies.

This study explores how Aripiprazole protects against CIRI and improves cerebral blood flow autoregulation function by inhibiting the p38 MAPK signaling pathway. Through a series of *in vivo* experiments, this study evaluated the protective effects of Aripiprazole using a rat model of cerebral ischemia-reperfusion, including its impact on cerebral infarction volume, brain edema, neurological function injury, and its regulatory impact on the p38 MAPK signaling pathway. Additionally, this study investigated the effect of Aripiprazole on cerebral blood flow autoregulation function and its potential underlying mechanisms. The anticipated outcomes of this study hold promise for providing new strategies and targets for treating CIRI, with significant clinical implications for improving patient outcomes.

Materials and Methods

Animal Treatments

Male Sprague-Dawley rats (n = 40), weighing 300 g and aged 8 weeks, were obtained from JACKSON LABORATORY (Shanghai, China). The rats were housed in controlled conditions with unrestricted access to food and water at a room temperature of 20 ± 1 °C. The study design was approved by the Ethics Review Committee of the Shandong First Medical University (no. 2023087). After a 1-week acclimatization period, the rats were randomly divided into four groups (n = 10/group) using a random number table method: (1) the I/R group, in which I/R rat models were constructed by middle cerebral artery occlusion (MCAO) and reperfusion, (2) the sham group, (3) the Aripiprazole+I/R group, in which rats received intraperitoneal injections of Aripiprazole (1 and 3 mg/kg; SML0935, 129722-12-9, Sigma-Aldrich, Bellefonte, PA, USA) [17], followed by the I/R model construction after 30 minutes, and (4) the Aripiprazole+I/R+Virodhamine group, in which rats received intraperitoneal injections of Aripiprazole (1 mg/kg) and an intravenous injection of p38 MAPK activator Virodhamine (HY-116418; 1 mg/kg; MedChemExpress, Monmouth Junction, NJ, USA) [18], followed by the I/R model construction after 30 minutes. During I/R model construction, rats were initially anesthetized using the intraperitoneal injection of sodium pentobarbital (50 mg/kg; P3761, Sigma-Aldrich, Bellefonte, PA, USA), the neck was dissected in the middle, exposing the left external carotid artery (ECA). The left cerebral artery was blocked by inserting a nylon thread into the internal carotid artery through the ECA. After 2 hours, the thread was removed, and the ECA wound was sutured. Rats were allowed to recover from anesthesia at room temperature. However, rats in the sham group underwent the same procedures except for thread insertion.

Neurological Deficits Assessment

After 24 hours of reperfusion, neurological impairments were evaluated by two researchers who were unaware of the experimental groups. Garcia's scale served as the primary evaluation tool, comprising 6 items with four levels each: behavioral scoring, neurofunctional assessment, motor function testing, and cognitive behavioral testing [19].

Brain Tissue Collection

After examining neurological deficits, rats were euthanized through inhalation of carbon dioxide (50% concentration), and their brain tissues were collected. In each experimental group, 3 brains were used for assessing brain water content (BWC), 3 brains were prepared for Triphenyltetrazolium Chloride (TTC) assay, and 4 brains were prepared as follows: portions of tissues were immediately frozen into liquid nitrogen and stored at –80 °C, while tissues from the striatum were immediately immersed in 4% paraformaldehyde (P0099, Beyotime, Shanghai, China) and 0.01 M phosphate-buffered saline (PBS; C0221A, Beyotime, Shanghai, China) for 5 days. After this, brain tissues were embedded in paraffin and subsequently sliced into 5-μm thickness sections. A part of the MCA and its branches were dissected to assess middle cerebral artery relaxation and vascular endothelium relaxation following a previously described method [20].

Assessment of Cerebral Edema

Cerebral edema was assessed through BWC measurement. The wet weight (WW) was measured using an electronic balance (02202101, Fisher Scientific, Shanghai, China). Subsequently, the brains were desiccated at 100 °C for 15 hours, and their dry weight was recorded. The BWC was calculated as 100% × (wet weight – dry weight)/wet weight.

TTC Assay and Quantification of Brain Infarct Volume

Brain samples were sliced into 2-mm coronal sections and immersed in a TTC solution (T8170, Solarbio, Beijing, China; dissolved in PBS) for 15 minutes at 37 °C in the

dark. Following fixation in 4% paraformaldehyde (P0099, Beyotime, Shanghai, China) for 24 hours, the sections were photographed. The brain infarction area was quantified using ImageJ software (version 1.48, National Institutes of Health, Rockville, MA, USA). The formula used to calculate infarct volume (%) is as follows: (contralateral hemisphere volume – the volume of the ipsilateral hemisphere without lesions) divided by (contralateral hemisphere volume multiplied by 2), then multiplied by 100% [21].

Hematoxylin-Eosin (H&E) Staining

The fixed tissue sections were dehydrated and cleared before being immersed in a staining solution containing hematoxylin-eosin (C0105S, Beyotime, Shanghai, China). Hematoxylin stains cell nuclei with a blue-purple hue, whereas eosin imparts a pink coloration to cytoplasm and intercellular spaces. Finally, the sections underwent dehydration, fixation, and mounting to prepare for microscopic observation (CK31, OLYMPUS, Tokyo, Japan).

Nissl Staining

The fixed neural tissue samples were sliced into sections ranging from 30 to 50 micrometers in thickness. These sections were then immersed in a Nissl staining solution (C0117, Beyotime, Shanghai, China), such as cresyl violet (10009128, Sinopharm Chemical Reagent Co., Ltd., Shanghai, China), to stain cell nuclei and cytoplasm. Following staining, the sections underwent washing to remove excessive dye and dehydration through increasing ethanol concentrations. Finally, the sections were fixed in a clearing agent and mounted onto glass slides for observation under a microscope (BX51, Olympus, Tokyo, Japan). Finally, the quantification of Nissl-positive cells was conducted using ImageJ software (version 1.48, National Institutes of Health, Rockville, MA, USA).

Brain Slice Method

Assessment of arterial dilation and constriction, as well as vascular endothelium, in the rat brain, was conducted using the Brain Slice Method [22]. The rat's head was secured on a frozen platform, and the brain was excised. The brain tissue was cooled and kept moist using ice-cold physiological saline solution or artificial cerebrospinal fluid (aCSF). Subsequently, the brain tissues were sliced into thin sections using a microtome, typically with a thickness of around 200 μm. These sections were then transferred to a dish containing chilled physiological saline solution. After this, the brain sections were placed in a warmed dish, and the baseline status of brain blood vessels was observed using a microscope (CX53, Olympus, Tokyo, Japan). Data analysis involved evaluating the dilation and constriction of blood vessels, followed by statistical analysis.

Table 1. A list of primers used in qRT-PCR.

Primer name	Primer sequence (5′-3′)
Rat *Bax*	F: GGGTGGTTGCCCTTTTCTACT
	R: AGTCCAGTGTCCAGCCCATG
Rat *Bcl-2*	F: ATCCAGGATAACGGAGGCTG
	R: CAGGTATGCACCCAGAGTGA
Rat *GAPDH*	F: ATGACTCTACCCACGGCAAG
	R: CTGGAAGATGGTGATGGGTT

Bcl-2, apoptosis regulator Bcl-2; *Bax*, Bcl-2 associated X; *GAPDH*, glyceraldehyde-3-phosphate dehydrogenase; F, forward; R, reverse.

qRT-PCR

Total RNA was extracted from the sample (R0016, Beyotime, Shanghai, China), followed by reverse transcription into complementary DNA (cDNA) (KR116, Tiangen, Beijing, China). Specific primers and DNA polymerase were used to amplify the cDNA of the target genes. Fluorescent probes or dyes were introduced during PCR (LightCycler96, Roche, Shanghai, China) to enable real-time detection of accumulated PCR products. The relative expression levels of the target gene in different samples were determined by comparing the fluorescence signals of samples with those of control groups. Finally, the expression levels of the target gene under various conditions were interpreted based on the results of the analysis. Quantitative analysis of the data was performed using the $2^{-\Delta\Delta Ct}$ method. The primer sequences are shown in Table 1.

Western Blot

Total protein was extracted from brain tissue samples using lysis buffer, supplemented with protease inhibitors (ST505, Beyotime, Shanghai, China). Before being resolved through sodium dodecyl sulfate-polyacrylamide gel electrophoresis (SDS-PAGE, P0012A, Beyotime, Shanghai, China), the proteins were quantified using the bicinchoninic acid (BCA) protein assay kit (P0012, Beyotime, Shanghai, China), and subsequently transferred onto a polyvinylidene difluoride (PVDF) membrane (IPVH00010, Millipore, Billerica, MA, USA). The PVDF membrane was blocked with 5% nonfat milk for 2 hours at room temperature. The membrane was incubated overnight with primary antibodies at 4 °C. Primary antibodies used in Western blot analysis were as follows: anti-phosphorylated p38 (1:1500 dilution; ab178867, Abcam, Cambridge, MA, USA), anti-p38 (1:1000 dilution; ab170099, Abcam, Cambridge, MA, USA), anti-ERK (1:1000 dilution; SC-271269, Santa Cruz Biotechnology, Inc., Santa Cruz, CA, USA), anti-JNK (1:1000 dilution; SC-7345, Santa Cruz Biotechnology, Inc., Santa Cruz, CA, USA), anti-p-ERK (1:1000 dilution; SC-7383, Santa Cruz Biotechnology, Inc., Santa Cruz, CA, USA), anti-p-JNK (1:1000 dilution; SC-81502, Santa Cruz Biotechnology, Inc., Santa Cruz, CA, USA), anti-Bcl-2 as-

Journal of
BIOLOGICAL REGULATORS
and Homeostatic Agents

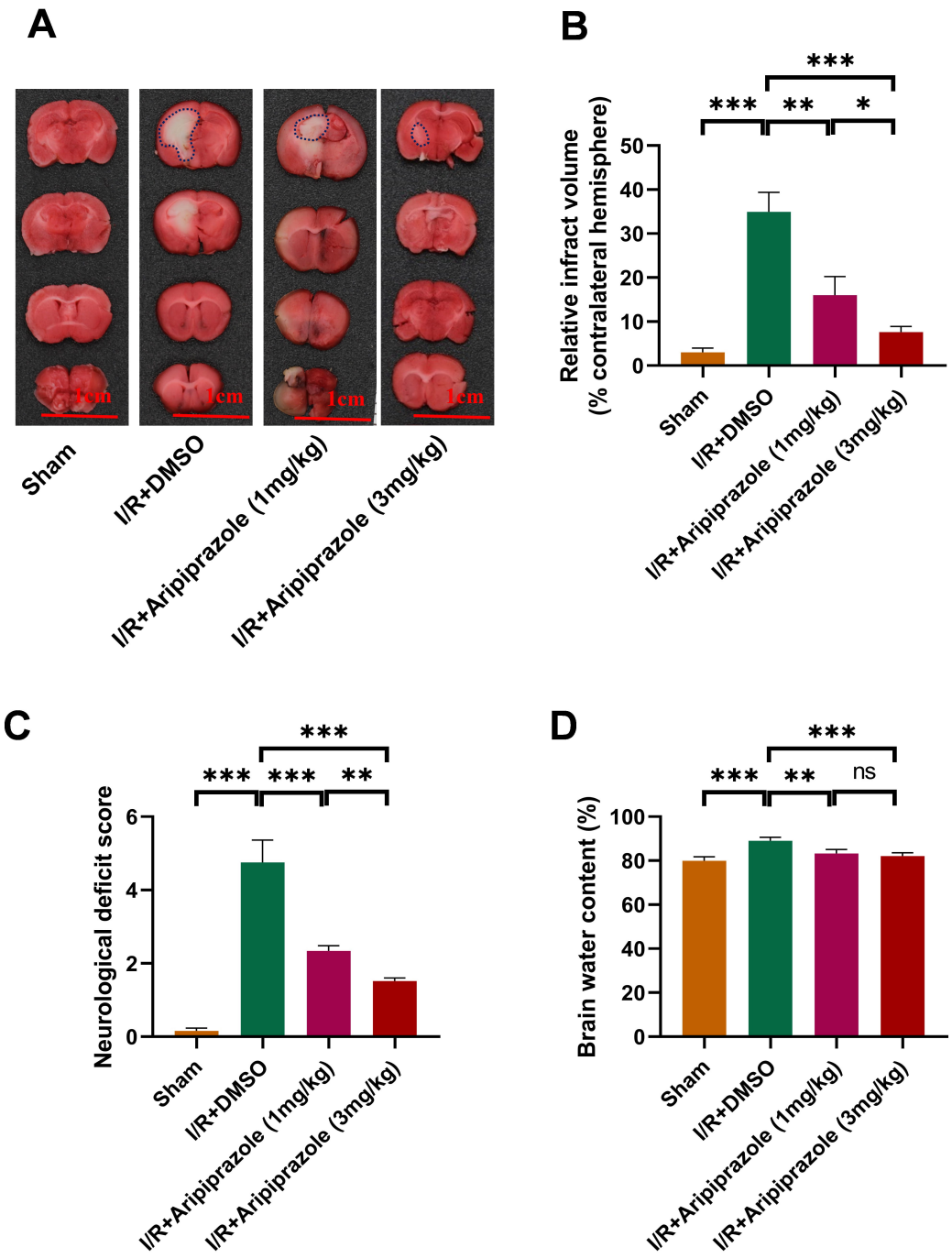

Fig. 1. Protective effects of Aripiprazole on neurological function, cerebral infarction, and brain edema after cerebral ischemia-reperfusion injury (CIRI) in rats. (A) Representative Triphenyltetrazolium Chloride (TTC) staining results of cerebral infarction. The dashed area represents the region of brain tissue damage. (B) Volume of cerebral infarction. (C) Assessment of impaired neurological function. (D) Measurement of brain water content. N = 10. $^{*}p < 0.05$, $^{**}p < 0.01$, $^{***}p < 0.001$, ns, no statistical difference.

sociated X (anti-Bax) (1:1500 dilution; MA5-14003, Invitrogen, Carlsbad, CA, USA), anti-apoptosis regulator Bcl-2 (anti-Bcl-2) (1:1500 dilution; MA5-11757, Invitrogen, Carlsbad, CA, USA), anti-β-actin (1:2000 dilution; ab6276, Abcam, Cambridge, MA, USA), and anti- glyceraldehyde-3-phosphate dehydrogenase (anti-GAPDH) (1:2000 dilution; ab8245, Abcam, Cambridge, MA, USA). After washing, the membranes were incubated with horseradish peroxidase (HRP)-conjugated secondary antibody (1:2000 dilution; ab7090, Abcam, Cambridge, MA, USA) for 2 hours at room temperature. Protein bands were visualized using the enhanced chemiluminescence kit (P0018S, Beyotime, Shanghai, China) and analyzed with ImageJ software (version 1.48, National Institutes of Health, Rockville, MD, USA).

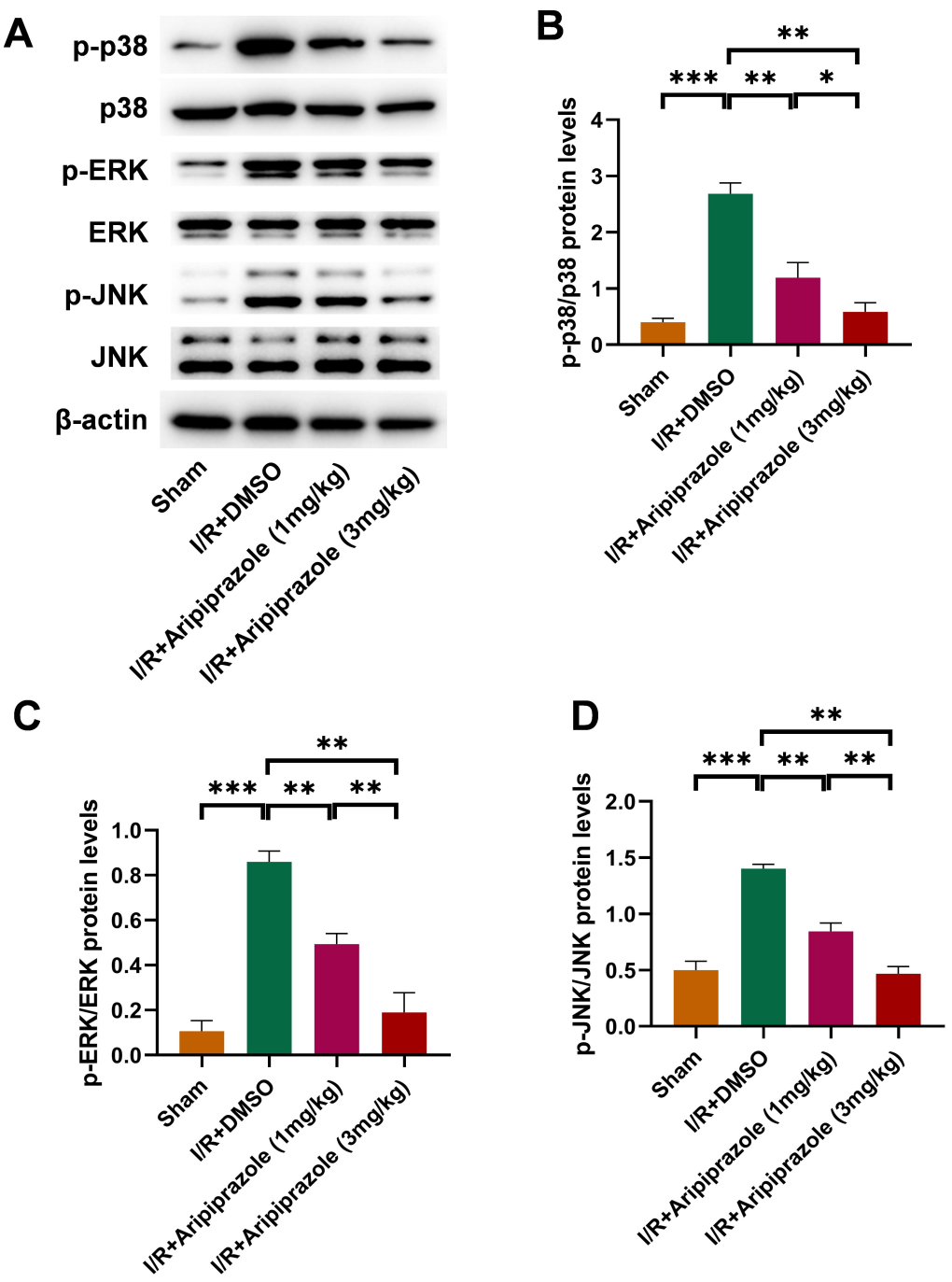

Fig. 2. Activation of the p38 mitogen-activated protein kinase (MAPK) signaling pathway by CIRI and its inhibition by Aripiprazole. (A–D) Analysis and statistical chart of the p38 MAPK signaling pathway-related protein expression using western blot analysis. N = 10. $^{*}p < 0.05$, $^{**}p < 0.01$, $^{***}p < 0.001$.

Terminal Deoxynucleotidyl Transferase dUTP Nick End Labeling (TUNEL)

Brain tissue sections, with about 40 µm thickness, were obtained from storage at –80 °C and processed. The sections were fixed in 4% paraformaldehyde (P0099, Beyotime, Shanghai, China) and permeabilized using proteinase K (P9460, Solarbio, Beijing, China). TUNEL labeling was performed using a kit (C1082, Beyotime, Shanghai, China), followed by DAPI staining at room temperature to visualize nuclei. Fluorescent labeling was observed using a fluorescence microscope (CKX53, OLYMPUS, Tokyo, Japan). Furthermore, apoptotic cells were counted in four randomly selected fields of view to assess their average. Quantitative analysis of apoptotic cells within the field of view was conducted using Image J software (version 1.48, National Institutes of Health, Rockville, MA, USA).

Journal of
BIOLOGICAL REGULATORS
and Homeostatic Agents

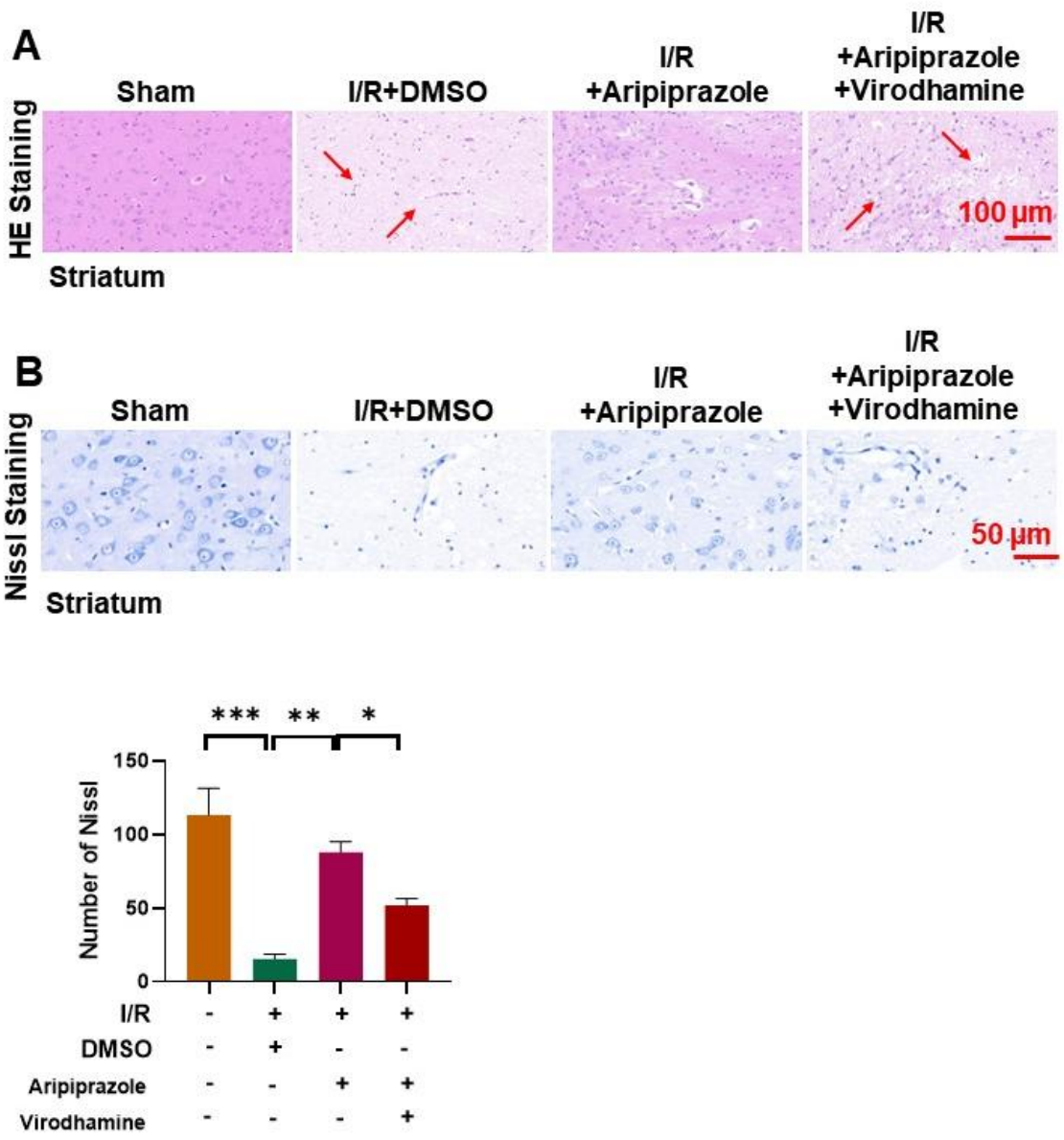

Fig. 3. Aripiprazole mitigated pathological changes in Ischemia/Reperfusion (I/R) brain tissue by inhibiting the p38 MAPK pathway. Activation of the MAPK pathway reversed the protective effects of Aripiprazole. (A) Representative images of hematoxylin-eosin (H&E) staining in the striatal region of the mouse brain. The red arrows indicate areas of tissue damage and cellular injury. (B) Results of Nissl staining in the striatum. N = 10. $^{*}p < 0.05$, $^{**}p < 0.01$, $^{***}p < 0.001$.

Enzyme-Linked Immunosorbent Assay (ELISA)

Total protein was extracted from tissue samples using the appropriate method and subsequently underwent quantification employing a protein quantification assay kit. The required reagents and assay kits were prepared according to the instructions provided with the corresponding ELISA kits, including interleukin (IL)-1β (EK201B, MultiSciences, Hangzhou, China), tumor necrosis factor-alpha (TNF-α; ab100747, Abcam, Cambridge, MA, USA), IL-6 (ab234570, Abcam, Cambridge, MA, USA), superoxide dismutase (SOD; ab65354, Abcam, Cambridge, MA, USA), malondialdehyde (MDA; ab233471, Abcam, Cambridge, MA, USA), and glutathione (GSH; S0053, Beyotime, Shanghai, China). Furthermore, a series of standard solutions at different concentrations were applied to construct a standard curve. Meanwhile, the extracted protein samples were appropriately diluted to match the concentrations of the standard solutions, as recommended in the assay kit instructions. Following the assay kit instructions, the diluted standard solutions, samples, and controls were sequentially added to the wells of the ELISA plate. The ELISA plate was shaken or oscillated to ensure a thorough reaction between the samples and the detection antibodies.

Finally, the optical density of the reaction products was assessed using an ELISA plate reader (KC; EMCXCL1, Invitrogen, Carlsbad, CA, USA).

Statistical Analysis

Statistical analysis was performed using GraphPad Prism software (version 8.0.2, GraphPad Software, La Jolla, CA, USA). Data were presented as mean ± standard deviation (SD). Each figure represents data from at least three independent experiments. The student's *t*-test was utilized to assess differences between two experimental groups, while ANOVA with the Student-Newman-Keuls test was applied for comparisons involving three or more groups. Statistical significance was defined as $p < 0.05$.

Results

Effect of Aripiprazole on Neurological Function, Cerebral Infarct, and Brain Water Content in Rats with CIRI

Following 24 hours of reperfusion, we employed TTC staining to assess the amount of the brain infarct. We observed that the infarct volume in the Aripiprazole (3 mg/kg)+I/R model group decreased by approximately 27% compared to the I/R model group ($p < 0.001$, Fig. 1A,B). However, rats in the I/R model group demonstrated a severe motor behavioral deficit evidenced by a significant increase in neurological deficiency ($p < 0.001$, Fig. 1C). Following cerebral I/R, rats treated with Aripiprazole showed a substantial decrease in neurological scores in a dose-dependent manner compared to the I/R model group ($p < 0.01$, Fig. 1C). Using the brain water content (BWC) assay, we determined the impact of Aripiprazole on the prognosis of cerebral ischemia in rats. As shown in Fig. 1D, the brain water content was significantly increased in the I/R group ($p < 0.001$) compared to the sham group. However, this effect was reversed following Aripiprazole treatment ($p < 0.01$). These findings suggest that Aripiprazole can promote the recovery process of cerebral ischemia.

Activation of the p38 MAPK Signaling Pathway in Cerebral I/R Model

We used western blot to examine the protein expression levels of p38 MAPK and p-p38 MAPK in the ischemic penumbra following 24 hours of reperfusion, aiming to determine the effects on the p38 MAPK pathway in the I/R brain. As presented in Fig. 2, compared to the sham group, the I/R group exhibited increased expression levels of p-p38, p-ERK, and p-JNK ($p < 0.01$). Conversely, the elevated p38 MAPK pathway was suppressed by Aripiprazole in the Aripiprazole+I/R group ($p < 0.01$). Furthermore, the degree of inhibition increased with increasing dose of Aripiprazole.

Aripiprazole Alleviated Pathological Changes in I/R Brain Tissues by Suppressing the p38 MAPK Pathway

H&E staining is a widely utilized technique for observing morphological features and pathological changes within tissues. The results demonstrated that the Sham group exhibited the least brain tissue damage, indicating a normal state unaffected by CIRI. The extent of damage observed in the I/R+Aripiprazole group was substantially lower than that in both the I/R+DMSO and I/R+Aripiprazole+Virodhamine groups (Fig. 3A). This outcome indicates that Aripiprazole can mitigate brain tissue damage induced by I/R. However, this protective effect was counteracted by the activation of the MAPK pathway by Virodhamine.

Furthermore, Nissl staining is a specific method used to identify and count Nissl bodies within neuronal cells and serves to assess neuronal health status. The Sham group showed the highest number of Nissl-positive cells, indicating good cellular health. The number of positive cells in the I/R+Aripiprazole group was higher than that in both the I/R+DMSO and I/R+Aripiprazole+Virodhamine groups (Fig. 3B, $p < 0.01$). This outcome suggests that Aripiprazole can protect neurons from I/R injury to a certain extent. However, when Aripiprazole combined with Virodhamine, this protective effect is reversed, leading to neuronal damage similar to that in the I/R-treated group. These results indicate that Aripiprazole effectively reduces brain I/R injury by inhibiting the p38 MAPK signaling pathway, thereby protecting neuronal cells. However, the activation of the p38 MAPK signaling pathway by Virodhamine counteracts the protective effect of Aripiprazole. These findings underscore the critical role of the p38 MAPK signaling pathway in brain I/R injury.

Aripiprazole Reduced Cell Apoptosis in I/R Brain Tissues by Suppressing the p38 MAPK Pathway

The apoptosis rate was assessed through immunofluorescence labeling with TUNEL. We observed that I/R damage increased the number of TUNEL-positive cells in the striatum ($p < 0.001$, Fig. 4A,B). In contrast, Aripiprazole treatment significantly reduced the proportion of TUNEL-positive cells compared to the I/R group ($p < 0.01$). Additionally, p38 MAPK activator substantially increased the cellular apoptosis rate ($p < 0.01$). These findings were further validated by evaluating the apoptosis-related mRNA expression (Fig. 4C,D), indicating that the Bax was upregulated, and Bcl-2 was downregulated in I/R ($p < 0.001$). However, regulation of Bax/Bcl-2 expression was reversed following Aripiprazole treatment ($p < 0.01$, $p < 0.001$). Similarly, the p38 MAPK activator counteracted their upregulation or downregulation in Aripiprazole-treated I/R model rats ($p < 0.05$, and $p < 0.01$ Fig. 4E-G). These results imply that Aripiprazole decreases cell apoptosis in brain tissues with I/R injuries by suppressing the p38 MAPK pathway.

Journal of
BIOLOGICAL REGULATORS
and Homeostatic Agents

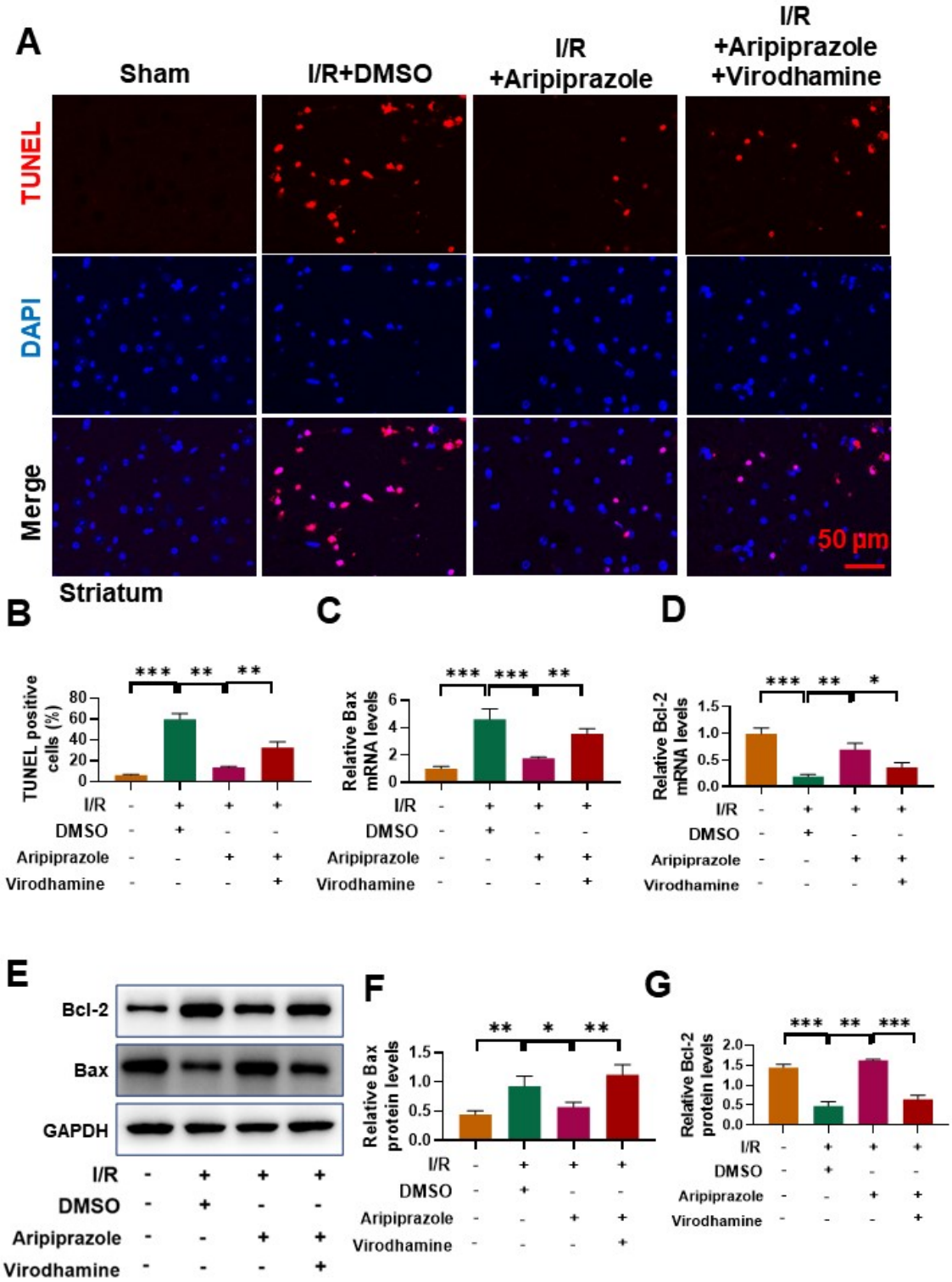

Fig. 4. Aripiprazole reduced cell apoptosis in I/R brain tissue by inhibiting the p38 MAPK pathway. (A,B) Detection of apoptosis using terminal deoxynucleotidyl transferase dUTP Nick End Labeling (TUNEL) immunofluorescence staining (scale bar: 50 μm). (C,D) mRNA expression levels of the apoptosis-related genes Bax (C) and Bcl-2 (D). (E–G) Protein expression levels of the apoptosis-related genes Bax and Bcl-2. N = 10. $^{*}p < 0.05$, $^{**}p < 0.01$, $^{***}p < 0.001$.

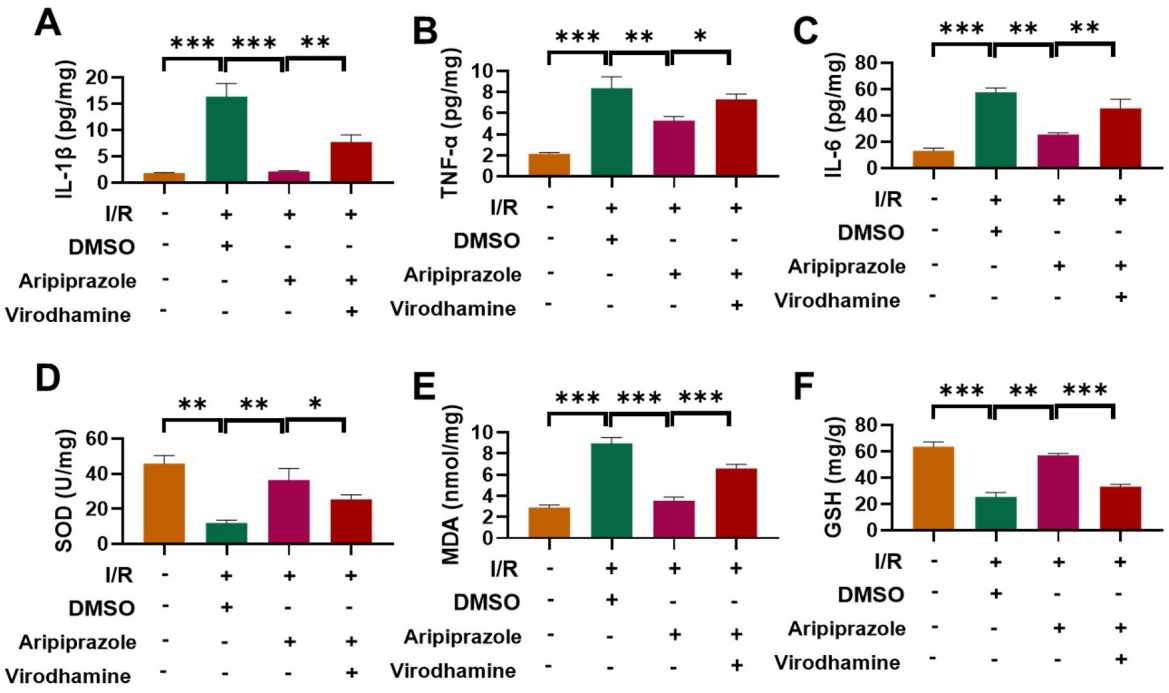

Fig. 5. Aripiprazole inhibited inflammation and oxidative stress in I/R brain tissue by suppressing the p38 MAPK pathway. (A–C) Protein levels of pro-inflammatory cytokines interleukin (IL)-1β (A), tumor necrosis factor-alpha (TNF-α) (B), and IL-6 (C) were determined using Enzyme-Linked Immunosorbent Assay (ELISA). (D–F) Superoxide dismutase (SOD) (D), malondialdehyde (MDA) (E), and glutathione (GSH) (F) levels were assessed utilizing ELISA. N = 10. $^{*}p < 0.05$, $^{**}p < 0.01$, $^{***}p < 0.001$.

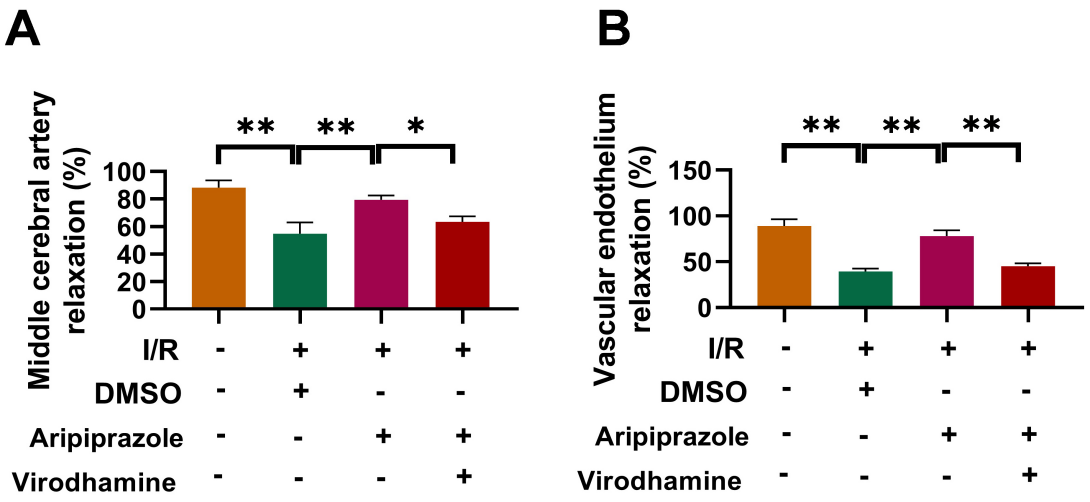

Fig. 6. Aripiprazole relaxed the middle cerebral artery and dilated the vascular endothelium in I/R rats by inhibiting the p38 MAPK pathway. (A) Relaxation of the rat's middle cerebral artery. (B) Role of vascular endothelium in the relaxation induced by Aripiprazole. N = 10. $^{*}p < 0.05$, $^{**}p < 0.01$.

Aripiprazole Inhibited Inflammation and Oxidative Stress in I/R Brain Tissues by Suppressing the p38 MAPK Pathway

As depicted in Fig. 5A–C, Aripiprazole treatment decreased the levels of I/R-promoted pro-inflammation cytokines IL-1β, TNF-α, and IL-6 ($p < 0.001$), which were reversely promoted by the p38 MAPK activator ($p < 0.05$, and $p < 0.01$). Moreover, the oxidative stress-related SOD and GSH were decreased while MDA was increased in the I/R group ($p < 0.01$, and $p < 0.001$). However, these effects were reversed following Aripiprazole treatment (Fig. 5D–F, $p < 0.05$, and $p < 0.001$). Furthermore, the p38 MAPK activator disrupted the reversing effect of Aripiprazole ($p < 0.05$, and $p < 0.001$). These findings indicate that Aripiprazole suppresses the I/R-induced inflammatory response and oxidative stress by suppressing the p38 MAPK pathway.

Journal of
BIOLOGICAL REGULATORS
and Homeostatic Agents

Aripiprazole Relaxed the Middle Cerebral Artery and Expanded Vascular Endothelium in I/R Rats by Suppressing the p38 MAPK Pathway

We sought to demonstrate that Aripiprazole induces vascular endothelial relaxation, impacting cerebral blood flow. Both middle cerebral artery relaxation (Fig. 6A) and vascular endothelium relaxation (Fig. 6B) were decreased by I/R ($p < 0.01$) but were reversely increased by Aripiprazole ($p < 0.01$). However, the Aripiprazole-induced reversing effect was disrupted by the p38 MAPK activator ($p < 0.05$, and $p < 0.01$), indicating that Aripiprazole regulates cerebral blood flow by suppressing the p38 MAPK pathway.

Discussion

This study delves into the neuroprotective role of Aripiprazole in a CIRI model and its underlying mechanisms. Through a series of experimental validations, we found that Aripiprazole significantly improves neurological functions post-I/R and reduces cerebral infarction volume and brain edema. These effects are closely associated with its ability to inhibit the p38 MAPK signaling pathway. Furthermore, Aripiprazole mitigates pathological changes in brain tissue induced by I/R, reduces cell apoptosis, inhibits inflammation and oxidative stress responses, and enhances cerebral blood flow autoregulation function. These findings provide significant experimental evidence for applying Aripiprazole in treating CIRI.

The p38 MAPK signaling pathway is pivotal in various cellular stress responses, including inflammation, cell apoptosis, and autophagy [23–25]. In CIRI, the activation of p38 MAPK is recognized as a crucial mechanism leading to neuronal cell damage [26,27]. Our findings demonstrate that Aripiprazole effectively inhibits the activation of the p38 MAPK signaling pathway induced by I/R, consistent with previous research findings. These observations further underscore the significant role of the p38 MAPK pathway in CIRI and suggest that Aripiprazole may exert neuroprotective effects by inhibiting this pathway.

Cell apoptosis is one of the primary forms of neuronal cell death in CIRI [5]. This study found that Aripiprazole significantly reduces cell apoptosis induced by I/R, possibly by inhibiting the p38 MAPK signaling pathway, thereby affecting the expression of apoptosis-related proteins, such as decreasing Bax expression and increasing Bcl-2 expression [28]. These results suggest that Aripiprazole exerts protective effects by regulating the expression of apoptosis-related genes and reducing cell apoptosis.

Moreover, inflammation and oxidative stress are two additional crucial mechanisms in CIRI. Our findings indicate that Aripiprazole significantly inhibits the inflammatory response and oxidative stress triggered by I/R, which may be linked to its suppression of the p38 MAPK signaling pathway, thereby reducing the production of pro-inflammatory cytokines and oxidative stress responses. These findings further confirm the role of Aripiprazole in inhibiting inflammation and oxidative stress, providing a new mechanistic explanation for its application in treating CIRI.

Moreover, this study revealed that Aripiprazole improves cerebral blood flow autoregulation following I/R, which may be potentially related to its ability to relax the middle cerebral artery and dilate vascular endothelium. The improvement of cerebral blood flow autoregulation function is crucial for maintaining blood supply to brain tissue and reducing ischemic damage. This discovery offers a new perspective on the potential application of Aripiprazole in improving cerebral blood flow.

Despite these significant findings, there are some limitations in this study. Firstly, the study primarily relies on animal models, and whether its results can be directly applied to humans requires further verification. Secondly, the mechanism through which Aripiprazole inhibits the p38 MAPK signaling pathway remains incompletely elucidated, warranting further molecular-level research. Additionally, the optimal dosage, timing window for administration, and the long-term efficacy and safety of Aripiprazole in treating CIRI require further investigation.

Conclusion

This study confirms that Aripiprazole effectively protects against CIRI and improves cerebral blood flow autoregulation function by inhibiting the p38 MAPK signaling pathway. These findings provide significant experimental evidence for the therapeutic application of Aripiprazole in treating CIRI and lay the foundation for further exploration of its mechanism of action and clinical application. Future research should focus on the specific mechanisms of action of Aripiprazole, the optimal treatment regimen, and its potential application in humans, aiming to provide new strategies for CIRI treatment.

Availability of Data and Materials

The datasets generated during and analysed during the current study are available from the corresponding authors on reasonable request.

Author Contributions

JHX and BM designed the research study; JZ and BM performed the research; PCL and TYZ collected and analyzed the data. BM and TYZ have been involved in drafting the manuscript. All authors have been involved in revising it critically for important intellectual content. All authors gave final approval of the version to be published. All authors have participated sufficiently in the work to take public responsibility for appropriate portions of the content and agreed to be accountable for all aspects of the work in ensuring that questions related to its accuracy or integrity.

Ethics Approval and Consent to Participate

The study design was approved by the Ethics Review Committee of the Shandong First Medical University (no. 2023087).

Acknowledgment

Not applicable.

Funding

This research received no external funding.

Conflict of Interest

The authors declare no conflict of interest.

References

[1] Liang TY, Peng SY, Ma M, Li HY, Wang Z, Chen G. Protective effects of sevoflurane in cerebral ischemia reperfusion injury: a narrative review. Medical Gas Research. 2021; 11: 152–154.

[2] Vongsfak J, Pratchayasakul W, Apaijai N, Vaniyapong T, Chattipakorn N, Chattipakorn SC. The Alterations in Mitochondrial Dynamics Following Cerebral Ischemia/Reperfusion Injury. Antioxidants. 2021; 10: 1384.

[3] Liao S, Apaijai N, Chattipakorn N, Chattipakorn SC. The possible roles of necroptosis during cerebral ischemia and ischemia / reperfusion injury. Archives of Biochemistry and Biophysics. 2020; 695: 108629.

[4] Chen SJ, Yuan XQ, Xue Q, Lu HF, Chen G. Current research progress of isoflurane in cerebral ischemia/reperfusion injury: a narrative review. Medical Gas Research. 2022; 12: 73–76.

[5] Zhang Q, Jia M, Wang Y, Wang Q, Wu J. Cell Death Mechanisms in Cerebral Ischemia-Reperfusion Injury. Neurochemical Research. 2022; 47: 3525–3542.

[6] Xu Y, Liu Y, Li K, Yuan D, Yang S, Zhou L, *et al*. COX-2/PGE2 Pathway Inhibits the Ferroptosis Induced by Cerebral Ischemia Reperfusion. Molecular Neurobiology. 2022; 59: 1619–1631.

[7] McGavin JK, Goa KL. Aripiprazole. CNS Drugs. 2002; 16: 779–786; discussion 787–788.

[8] Preda A, Shapiro BB. A safety evaluation of aripiprazole in the treatment of schizophrenia. Expert Opinion on Drug Safety. 2020; 19: 1529–1538.

[9] Kikuchi T, Maeda K, Suzuki M, Hirose T, Futamura T, McQuade RD. Discovery research and development history of the dopamine D_2 receptor partial agonists, aripiprazole and brexpiprazole. Neuropsychopharmacology Reports. 2021; 41: 134–143.

[10] Mohr P, Masopust J, Kopeček M. Dopamine Receptor Partial Agonists: Do They Differ in Their Clinical Efficacy? Frontiers in Psychiatry. 2022; 12: 781946.

[11] Yue J, López JM. Understanding MAPK Signaling Pathways in Apoptosis. International Journal of Molecular Sciences. 2020; 21: 2346.

[12] Li T, Wu YN, Wang H, Ma JY, Zhai SS, Duan J. Dapk1 improves inflammation, oxidative stress and autophagy in LPS-induced acute lung injury via p38MAPK/NF-κB signaling pathway. Molecular Immunology. 2020; 120: 13–22.

[13] Whitaker RH, Cook JG. Stress Relief Techniques: p38 MAPK Determines the Balance of Cell Cycle and Apoptosis Pathways. Biomolecules. 2021; 11: 1444.

[14] Zhao H, Deng L, Chen S, Wang X, Dong Z. Neuroprotection of β-caryophyllene against cerebral ischemia/reperfusion injury by inhibiting P38 MAPK/NLRP3 signaling pathway. Neuroreport. 2023; 34: 617–623.

[15] Zhang L, Sui R, Zhang L. Fingolimod protects against cerebral ischemia reperfusion injury in rats by reducing inflammatory cytokines and inhibiting the activation of p38 MAPK and NF-κB signaling pathways. Neuroscience Letters. 2022; 771: 136413.

[16] Xu D, Kong T, Shao Z, Liu M, Zhang R, Zhang S, *et al*. Orexin-A alleviates astrocytic apoptosis and inflammation via inhibiting OX1R-mediated NF-κB and MAPK signaling pathways in cerebral ischemia/reperfusion injury. Biochimica et Biophysica Acta. Molecular Basis of Disease. 2021; 1867: 166230.

[17] Sun YY, Zhu HJ, Zhao RY, Zhou SY, Wang MQ, Yang Y, *et al*. Remote ischemic conditioning attenuates oxidative stress and inflammation via the Nrf2/HO-1 pathway in MCAO mice. Redox Biology. 2023; 66: 102852.

[18] Mathew B, Ruiz P, Dutta S, Entrekin JT, Zhang S, Patel KD, *et al*. Structure-activity relationship (SAR) studies of N-(3-methylpyridin-2-yl)-4-(pyridin-2-yl)thiazol-2-amine (SRI-22819) as NF-κB activators for the treatment of ALS. European Journal of Medicinal Chemistry. 2021; 210: 112952.

[19] Garcia JH, Wagner S, Liu KF, Hu XJ. Neurological deficit and extent of neuronal necrosis attributable to middle cerebral artery occlusion in rats. Statistical validation. Stroke. 1995; 26: 627–634; discussion 635.

[20] Gaw AJ, Bevan JA. Flow-induced relaxation of the rabbit middle cerebral artery is composed of both endothelium-dependent and -independent components. Stroke. 1993; 24: 105–109; discussion 109–110.

[21] Jiang M, Li J, Peng Q, Liu Y, Liu W, Luo C, *et al*. Neuroprotective effects of bilobalide on cerebral ischemia and reperfusion injury are associated with inhibition of pro-inflammatory mediator production and down-regulation of JNK1/2 and p38 MAPK activation. Journal of Neuroinflammation. 2014; 11: 167.

[22] Kuts R, Frank D, Gruenbaum BF, Grinshpun J, Melamed I, Knyazer B, *et al*. A Novel Method for Assessing Cerebral Edema, Infarcted Zone and Blood-Brain Barrier Breakdown in a Single Post-stroke Rodent Brain. Frontiers in Neuroscience. 2019; 13: 1105.

[23] Chipurupalli S, Samavedam U, Robinson N. Crosstalk Between ER Stress, Autophagy and Inflammation. Frontiers in Medicine. 2021; 8: 758311.

[24] Wang L, Zhang X, Xiong X, Zhu H, Chen R, Zhang S, *et al*. Nrf2 Regulates Oxidative Stress and Its Role in Cerebral Ischemic Stroke. Antioxidants. 2022; 11: 2377.

[25] Li XH, Yin FT, Zhou XH, Zhang AH, Sun H, Yan GL, *et al*. The Signaling Pathways and Targets of Natural Compounds from Traditional Chinese Medicine in Treating Ischemic Stroke. Molecules. 2022; 27: 3099.

[26] Zhang Y, Zhang Z, Wang J, Zhang X, Zhao J, Bai N, *et al*. Scutellarin alleviates cerebral ischemia/reperfusion by suppressing oxidative stress and inflammatory responses via MAPK/NF-κB pathways in rats. Environmental Toxicology. 2022; 37: 2889–2896.

[27] Kong C, Miao F, Wu Y, Wang T. Oxycodone suppresses the apoptosis of hippocampal neurons induced by oxygen-glucose deprivation/recovery through caspase-dependent and caspase-independent pathways via κ- and δ-opioid receptors in rats. Brain Research. 2019; 1721: 146319.

[28] Niizuma K, Yoshioka H, Chen H, Kim GS, Jung JE, Katsu M, *et al*. Mitochondrial and apoptotic neuronal death signaling pathways in cerebral ischemia. Biochimica et Biophysica Acta. 2010; 1802: 92–99.